Stem Cell Reports
Report
OPEN ACCESS

Activating Endogenous Neural Precursor Cells Using Metformin Leads to Neural Repair and Functional Recovery in a Model of Childhood Brain Injury

Parvati Dadwal,[1,2,9] Neemat Mahmud,[2,3,9] Laleh Sinai,[2] Ashkan Azimi,[1,2] Michael Fatt,[1,4] Fredric E. Wondisford,[5] Freda D. Miller,[1,4,6,7] and Cindi M. Morshead[1,2,3,8,*]
[1]Institute of Medical Science, University of Toronto, 1 King's College Circle, Toronto, ON M5S 1A8, Canada
[2]Donnelly Centre, University of Toronto, 160 College Street, Toronto, ON M5S 3E1, Canada
[3]Department of Surgery, University of Toronto, 1 King's College Circle, Toronto, ON M5S 1A8, Canada
[4]Neuroscience and Mental Health Program, Hospital for Sick Children, Toronto, ON M5G 1X8, Canada
[5]Department of Medicine, Pediatrics and Physiology, Johns Hopkins University School of Medicine, Baltimore, MD 21287, USA
[6]Department of Molecular Genetics, University of Toronto, 1 King's College Circle, Toronto, ON M5S 1A8, Canada
[7]Department of Physiology, University of Toronto, 1 King's College Circle, Toronto, ON M5S 1A8, Canada
[8]Institute of Biomaterial and Biomedical Engineering, University of Toronto, 563 Spadina Crescent, Toronto, ON M5S 2J7, Canada
[9]Co-first author
*Correspondence: cindi.morshead@utoronto.ca
http://dx.doi.org/10.1016/j.stemcr.2015.06.011

SUMMARY

The development of cell replacement strategies to repair the injured brain has gained considerable attention, with a particular interest in mobilizing endogenous neural stem and progenitor cells (known as neural precursor cells [NPCs]) to promote brain repair. Recent work demonstrated metformin, a drug used to manage type II diabetes, promotes neurogenesis. We sought to determine its role in neural repair following brain injury. We find that metformin administration activates endogenous NPCs, expanding the size of the NPC pool and promoting NPC migration and differentiation in the injured neonatal brain in a hypoxia-ischemia (H/I) injury model. Importantly, metformin treatment following H/I restores sensory-motor function. Lineage tracking reveals that metformin treatment following H/I causes an increase in the absolute number of subependyma-derived NPCs relative to untreated H/I controls in areas associated with sensory-motor function. Hence, activation of endogenous NPCs is a promising target for therapeutic intervention in childhood brain injury models.

INTRODUCTION

Perinatal hypoxic-ischemic (H/I) insult is an important cause of brain injury and can result in long-term neurological complications, ranging from mild behavioral deficits to severe seizure, intellectual disability, and/or cerebral palsy. Neural injury results from excitotoxicity, inflammation, and oxidative stress, leading to a loss of oligodendrocytes and neurons, which are particularly sensitive to H/I (Deng, 2010). With the exception of rehabilitation, there are no established treatments available to improve behavioral deficits in these patients to date.

The development of cell replacement strategies to repair the injured brain has gained considerable attention, with a particular interest in mobilizing endogenous neural precursor cells (NPCs). Several studies have investigated the impact of H/I on the germinal zone, a region that contains multipotent NPCs. It has been shown that neural stem cells (NSCs) remain resilient to this insult (Romanko et al., 2004) and can regenerate neurons and oligodendrocytes following H/I, albeit to a very limited extent (Felling et al., 2006; Ong et al., 2005; Plane et al., 2004; Yang and Levison, 2006; Yang et al., 2007; Zaidi et al., 2004).This injury-induced activation leads to a rare fraction of cells migrating to the injury site, which is not sufficient for self-repair (Ikeda et al., 2005). With the goal of developing new methodologies to enhance NPC activation in the neonatal brain and promote neural repair following H/I, we have built on successful NPC activation strategies that lead to tissue formation and functional recovery using small molecules to mobilize endogenous NPCs (Erlandsson et al., 2011; Kolb et al., 2007). Previous work has demonstrated that atypical PKC-dependent phosphorylation of CREB-binding protein (CBP) on serine 436 is necessary for enhancing differentiation in cortical precursor cells (Wang et al., 2010). Moreover, this pathway is activated by metformin, an AMPK agonist, shown to promote neurogenesis and enhance spatial memory in uninjured mice (Wang et al., 2012). Based on these findings, we asked whether metformin could be used to stimulate subependyma (SE)-derived NPCs and promote repair of the H/I-injured neonatal murine brain.

RESULTS

Metformin Expands the Stem Cell Pool and Promotes Differentiation via the aPKC-CBP Pathway in Neonatal Pups, In Vitro

It is currently unknown whether metformin acts on the NSCs, their downstream progeny, or both that ultimately leads to enhanced neurogenesis. To test if metformin had

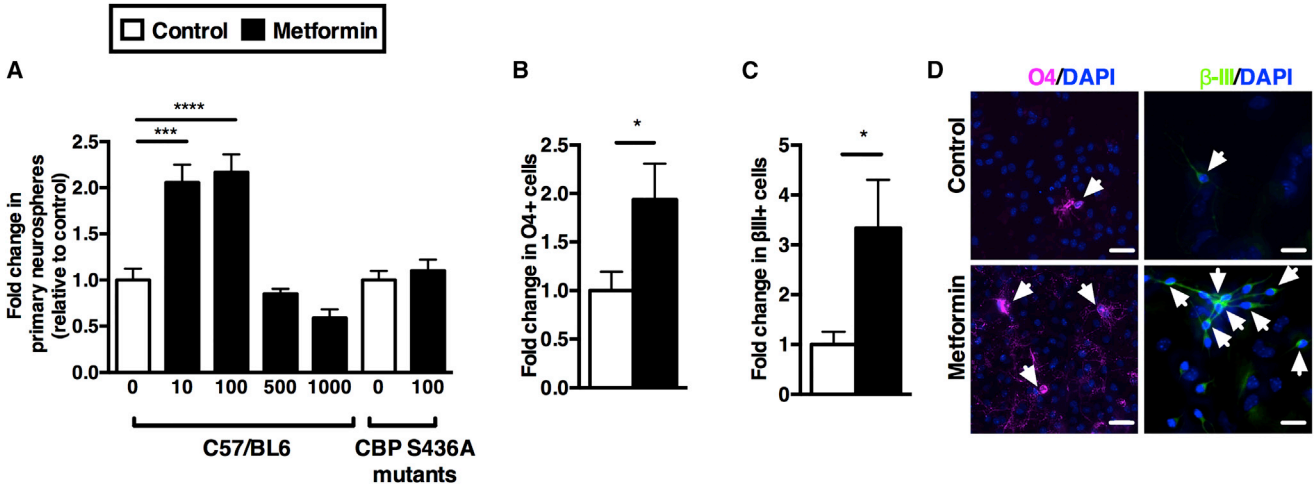

Figure 1. Metformin Increases the Stem Cell Pool and Promotes Differentiation via the aPKC-CBP Pathway in Neonatal Pups

(A) Metformin was added at various concentrations to SE-derived NPCs. Neurosphere numbers were assayed following 7 days in culture (n = 4 independent experiments, one-way ANOVA). In CBP S436A mutant mice, SE-derived NPCs were grown in either 0 ng/ml or 100 ng/ml metformin (n = 13 mice, t test).

(B) Fold increase of O4-positive oligodendrocytes is shown (n = 9/group, t test).

(C) Fold increase of βIII-tubulin-positive neurons within a neurosphere is shown (n = 5/group, t test).

(D) Immunostaining for O4 (purple), βIII-tubulin (green), and Hoechst (blue) in cultures in the absence or presence of metformin during the proliferation and differentiation phases is shown. Scale bars, 20 μm. Data are presented as mean ± SEM. *p < 0.05, ***p < 0.001, ****p < 0.0001.

direct effects on NSCs, we used an in vitro, colony-forming assay, termed the neurosphere assay on postnatal day 8 (P8) pups from C57/BL6 (control) and CBP S436A mice (CBP S436A mutants harboring a point mutation from serine to alanine in the CBP gene specifically at the aPKC phosphorylation site) (He et al., 2009). Phosphorylation at serine 436 has been shown to be essential for neural differentiation in embryonic precursors; hence, we predicted that direct effects of metformin on NPCs would not be seen in CBP S436A mutant mice. Briefly, the SE is dissected, dissociated, and plated into single cells. Over a period of 7 days, single NSCs proliferate to form a free-floating colony of cells known as a neurosphere. Each individual neurosphere is a mixed population of stem and progenitor cells (Morshead et al., 2002). In primary culture, an increase in the total numbers of neurospheres indicates an expansion of the stem cell pool. In the presence of metformin, we observed a significant (>2-fold) increase in the numbers of primary neurospheres in control mice, whereas this effect was lost in CBP S436A mutant mice (Figure 1A). Further, primary P8 SE-derived neurospheres grown and differentiated in culture in the presence of metformin gave rise to significantly more oligodendrocytes (1.9-fold increase) and neurons (3.3-fold increase) compared to controls (Figures 1B–1D), and this effect was lost for CBP S436A mutants cultured in the same conditions (data not shown). Thus, metformin expands the stem cell pool and promotes oligodendrogenesis and neurogenesis from the early postnatal brain via the aPKC-CBP pathway.

Functional Recovery in Injured Mice following Metformin Treatment

We asked if administration of metformin was able to enhance brain repair in a well-established model of neonatal brain injury (Vannucci and Vannucci, 2005; Vannucci et al., 1999). P8 pups received a left common carotid artery ligation followed by hypoxia for 1 hr. H/I-injured pups revealed sensory-motor deficits, with increased latencies in the righting reflex motor task and decreased latencies in the hind limb suspension task at 1 hr and 4 days post-H/I, respectively, when compared to uninjured pups (Figures 2A–2C; Figure S1). Metformin was delivered to neonatal pups starting 24 hr post-H/I via their lactating mothers, which had 7-day micro-osmotic pumps implanted subcutaneously (20 mg/kg/day), or by subcutaneous injection directly into the pups (20 mg/kg/day). We first assayed for the effects of H/I and/or metformin treatment on SE-derived NPC behavior. Uninjured pups that received metformin through the mother's milk for 4 days (from P9–12) had a 2-fold increase in the number of neurospheres (stem cell pool expansion), similar to what was observed in culture (Figure 1A). As predicted, subcutaneous metformin injections given to CBP S436A mutant mice did not result in expansion of the stem cell pool (Figure 2D).

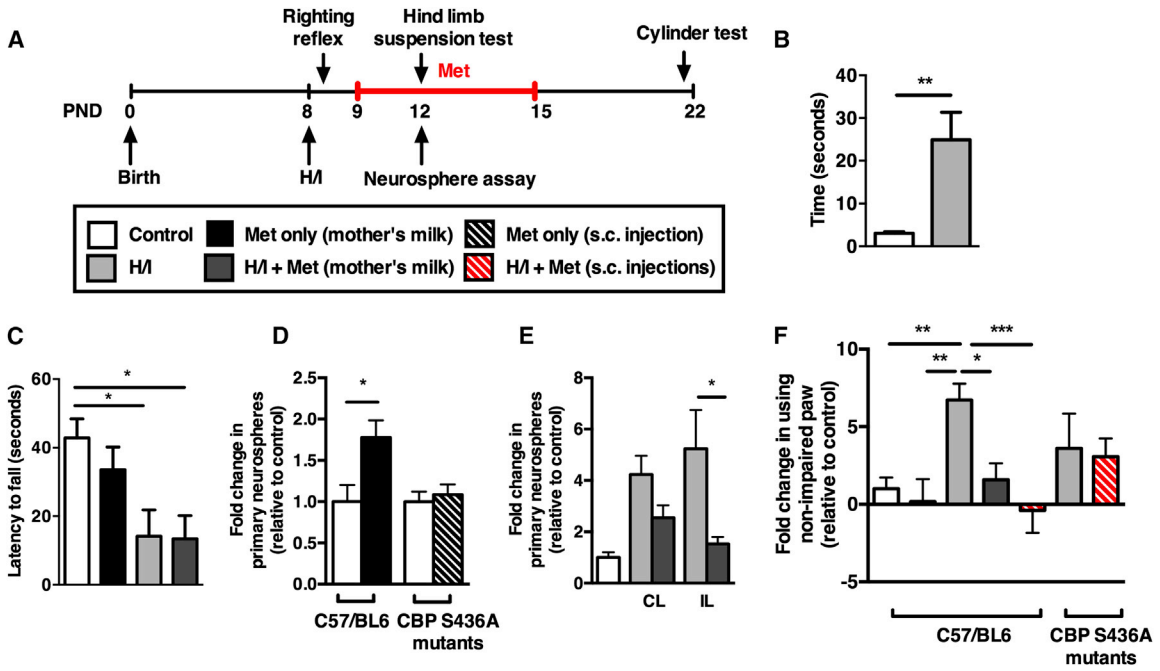

Figure 2. Metformin Treatment following Injury Rescues Motor Deficits, In Vivo

(A) Experimental paradigm of injury and metformin treatment. Metformin was administered 1 day following injury to lactating mothers.

(B) Mice were tested on their ability to flip from supine position to prone position 1 hr after H/I (n = 11 mice/group, t test).

(C) Latency to fall from the edge of the tube was compared between different treatment groups (n $\geq$ 6 mice/group, t test).

(D) Expansion of the SE-derived NPC pool in metformin-treated mice (n = 6 mice/group, t test). This metformin-induced expansion of the SE-derived NPC pool was lost in CBP S436A mutants (n $\geq$ 12 mice/group, t test).

(E) An H/I injury alone expanded the stem cell pool (n = 5 mice/group, two-way ANOVA).

(F) The cylinder-rearing test was used to assess sensory-motor function. Graph depicts non-impaired forepaw preference for mice tested on day 22 (n $\geq$ 7 mice/group, one-way ANOVA). Met, metformin; CL, contralateral hemisphere to ischemia; IL, ipsilateral hemisphere to ischemia. Data are presented as mean ± SEM. *p < 0.05, **p < 0.01.

See also Figure S1.

H/I injury alone increased the size of the NSC pool (≥4-fold increase) both ipsilateral (IL) and contralateral (CL) to the ischemic insult. Interestingly, H/I + metformin-treated pups gave rise to reduced numbers of SE-derived neurospheres relative to the H/I treatment (although similar to metformin-only-treated mice) (Figure 2E). One potential explanation for this relative decrease is that metformin promoted the migration of endogenous NPCs into the surrounding parenchyma. In support of this hypothesis, when we performed the neurosphere assay from cortical tissue, we observed a complete lack of neurospheres from control (uninjured) and metformin-only-treated mice, whereas neurospheres were consistently generated from the frontal cortices of H/I + metformin-treated pups (5.0 ± 2.5 neurospheres/cortices).

We then asked whether metformin treatment was able to promote functional recovery. Notably, 4 days of metformin treatment (P9–12) was not sufficient to improve the motor impairment in the hind-limb suspension task in H/I-injured pups (Figure 2C). In contrast, mice that received 7 days of metformin treatment (P9–15) displayed significant recovery in forelimb function when tested in the cylinder task 2 weeks after the lesion (P22) (Figure 2F). Mice that experienced H/I alone displayed a significant preference for use of the IL, unimpaired paw. Indeed, the performance of metformin-treated mice was not statistically different from uninjured controls. To ensure the functional recovery observed in metformin-treated mice was not due to secondary effects, H/I-injured pups received subcutaneous injections of metformin from P9–15. As was seen following exposure to metformin via the mother's milk, we observed recovery in metformin-injected H/I mice, indicating a direct effect of metformin. Next, we asked if this functional recovery was mediated by activation of the aPKC-CBP pathway. Most strikingly, CBP S436A mutants that received subcutaneous injections of metformin from P9–15 following H/I injury did not display functional recovery compared to CBP S436A

mutants that had an H/I injury (Figure 2F). Hence, metformin promoted functional recovery via the aPKC-CBP pathway.

Metformin Promotes Expansion, Migration, and Differentiation of Endogenous NPCs in the Injured Brain

To determine the cellular basis for this restored function on the sensory-motor task, we performed lineage-tracking experiments using *Nestin-CreER^{T2}/R26R-YFP* transgenic mice. When these mice are exposed to tamoxifen, this leads to recombination and expression of YFP in nestin-expressing NPCs and all of their progeny. To perform the lineage tracing, we provided tamoxifen to lactating mothers in their food chow, and thereby exposed their neonatal pups to tamoxifen shortly after birth. At P8, prior to H/I, the vast majority of YFP-positive cells were confined to the SE in the brains of these offspring (Figure S2A). Groups of tamoxifen-treated pups received H/I with or without metformin treatment and their brains were examined at P16 (immediately after metformin treatment, Figures S2B–S2F) and at P23 (time of observed functional recovery, Figure 3A). At both day 16 and 23, H/I + metformin-treated mice had more SE-derived YFP-positive cells in all areas examined, in both the IL and CL parenchyma. At the time of functional recovery (P23), H/I + metformin pups displayed significant increases in YFP-positive cells in the olfactory bulb and subventricular zone and an increasing trend in the hippocampus where NPCs and ongoing neurogenesis are normally observed (Figures S2G–S2K). Similarly, we observed significant increases in YFP-positive cells in regions of the brain known to play a role in motor activities (striatum, corpus callosum, and the motor cortex) compared to H/I-only- and metformin-only-treated mice (>4-fold in all areas) (Figures 3B and 3E). Indeed, H/I-only and metformin-only brains had very few YFP-positive cells in the parenchyma and were not significantly different from each other (Figure 3B).

We examined the differentiation profile of the SE-derived, YFP-positive cells by counting the numbers of neurons (YFP+/NeuN+) and oligodendrocytes (YFP+/MBP+ and YFP+/Olig2+). Neurogenesis and oligodendrogenesis were not significantly different in any region examined between H/I-only- and metformin-only-treated brains (Figures 3C and 3D). However, we consistently observed significantly increased numbers of differentiated cells in H/I + metformin-treated mice IL and CL to the lesion (Figures 3C–3G), with the exception of neurogenesis in the motor cortex. Most striking was the dramatic increase in oligodendrogenesis in H/I + metformin-treated mice in both hemispheres in the striatum (6-fold CL, 23-fold IL), motor cortex (10-fold CL, 6-fold IL), and corpus callosum (8-fold CL, 3-fold IL) (Figures 3D and 3G). The increased oligodendrocyte formation in H/I + metformin-treated mice was further assessed using western blots. As seen in Figure S2L, the level of MBP was markedly increased in the H/I + metformin group relative to control H/I.

To understand the effect of metformin underlying functional recovery, we analyzed the relative percentage of YFP+ cells that differentiated into oligodendrocytes and neurons in the striatum, corpus callosum, and motor cortex, between H/I- and H/I + metformin-treated brains (Figure 3H). Notably, while the total numbers of SE-derived, YFP+ cells within the brain parenchyma were dramatically different between H/I- and H/I + metformin-treated mice, we observed no difference in the relative percentage of differentiated cell types within the parenchyma. Further, we found the relative distribution of SE-derived YFP+ cells to be similar between H/I-only- versus H/I + metformin-treated brains, with the majority of cells found in the olfactory bulb (Figure S2M). Taken together, these findings suggest that it is the magnitude of the contribution of newborn cells to the brain tissue that correlates with the functional recovery observed in H/I + metformin-treated pups (Figure S2N).

DISCUSSION

Our findings indicate that endogenous NPC activation following injury is able to promote self-repair and functional recovery in a rodent model of childhood brain injury. We demonstrate metformin treatment in the neonatal brain for 7 days can lead to expansion and migration into the brain parenchyma of NPCs that play a role in sensory-motor function.

Drug therapy for the H/I-injured brain has focused largely on anti-oxidants (allopurinol, N-acetylcysteine), anti-excitotoxic agents (topiramate, memantine), and anti-inflammatory agents (cromolyn) (Juul and Ferriero, 2014; Hagberg et al., 2015). These therapies have been shown to primarily mediate their effects through neuroprotection and have resulted in varying degrees of functional recovery and a reduction in infarct volume. Further, while they display similarities in cost-effectiveness, implications in different injury models, and success in adults or old age animals, metformin is the only drug treatment that has demonstrated efficacy in generating new cells in the neonatal brain. Metformin may confer additional advantages such as improving lifespan (Martin-Montalvo et al., 2013) and promoting angiogenesis (Jin et al., 2014; Liu et al., 2014; Venna et al., 2014).

The finding that metformin, an anti-diabetic drug, increases the absolute number of NPCs following injury (rather than changing the relative percentage of differentiated cells) was surprising. Several possibilities could

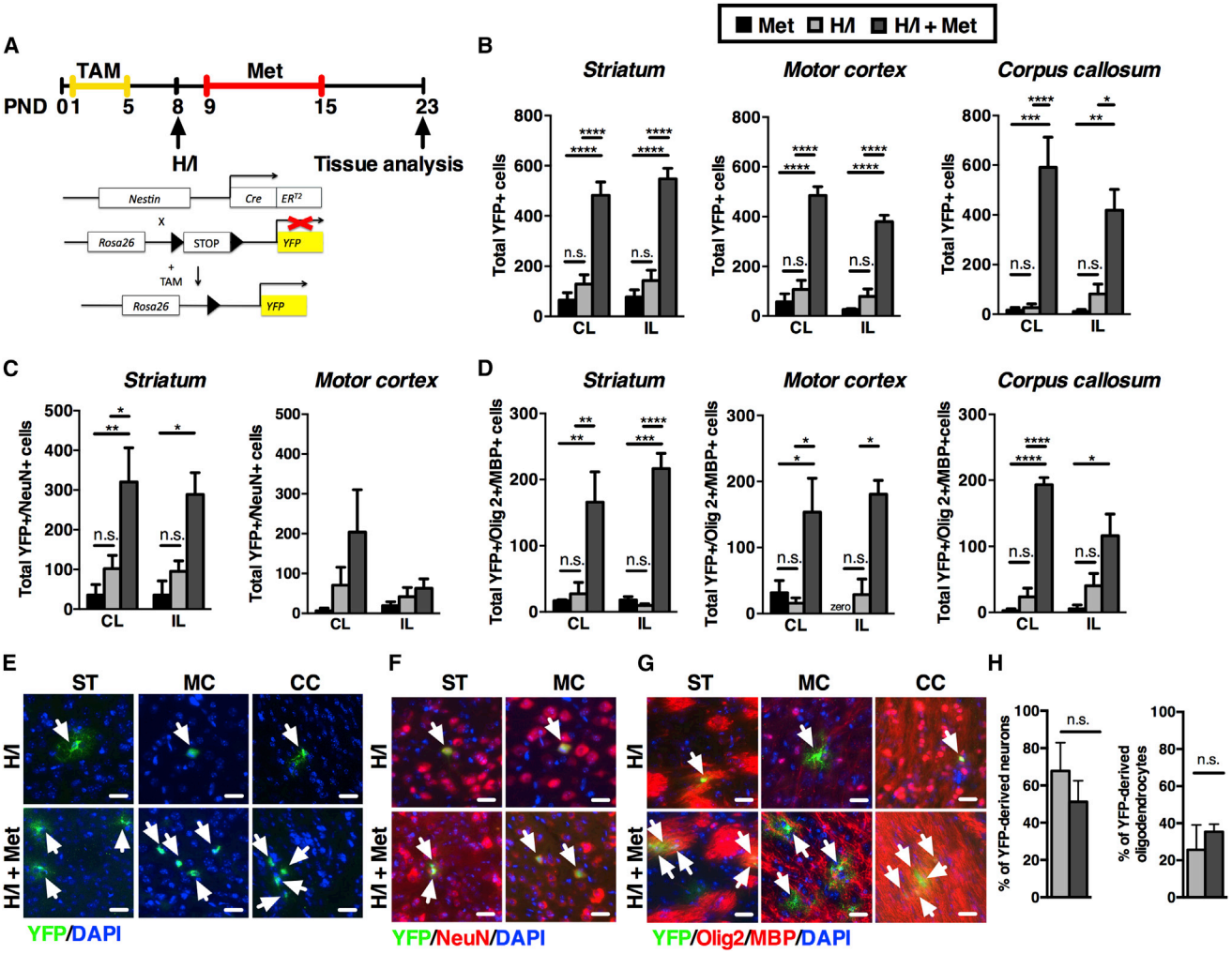

Figure 3. Metformin Increases the Absolute Numbers of SE-Derived NPCs in the Brain Parenchyma following Injury

(A) Experimental design for metformin administration and behavioral testing. Lineage tracing of SE-derived cells used *Nestin-CreER^{T2}/R26R-YFP* transgenic mice.

(B) Quantification of SE-derived YFP+ cells found in the striatum ($n \geq 3$ mice/group, two-way ANOVA), motor cortex ($n \geq 3$ mice/group, two-way ANOVA), and corpus callosum ($n \geq 3$ mice/group, two-way ANOVA) is shown.

(C) Quantification of YFP+ cells that were co-labeled with NeuN, indicating newborn neurons, in striatum ($n \geq 3$ mice/group, two-way ANOVA) and motor cortex ($n \geq 3$ mice/group, two-way ANOVA) is shown.

(D) Quantification of YFP+ cells that were co-labeled with Olig2+ or MBP+, indicating newborn immature or mature oligodendrocytes, respectively, in striatum ($n \geq 3$ mice/group, two-way ANOVA), motor cortex ($n \geq 3$ mice/group, two-way ANOVA), and corpus callosum ($n \geq 3$ mice/group, two-way ANOVA) is shown.

(E–G) Coronal sections immunostained for YFP+ cells (green) and Hoechst (blue) (E); YFP+ (green), NeuN (red), and Hoechst (blue) (F); and YFP+ (green), Olig2+/MBP+ (red), and Hoechst (blue) (G) are shown.

(H) The relative percentages of differentiated neurons (striatum and motor cortex) and differentiated oligodendrocytes (striatum, motor cortex, and corpus callosum) were not significantly different between groups. IL and CL hemispheres were pooled together ($n \geq 4$ mice/group, t test). Arrows denote labeled cells. Scale bars, 20 μm. Data are presented as mean ± SEM. TAM, tamoxifen; ST, striatum; MC, motor cortex; CC, corpus callosum. *$p < 0.05$, **$p < 0.01$, ***$p < 0.001$, ****$p < 0.0001$.

See also Figure S2.

account for this observation. For example, metformin could have direct effects on NPCs (such as changes in cell-cycle kinetics and/or promoting cell survival) or indirect effects on non-NPCs that leads to the release of growth/trophic factors, providing immunomodulation, neuroprotection, and/or angiogenesis, which could effectively lead to an

expansion in the size of the NPC pool. Indeed with respect to the latter, recent studies using chronic metformin treatment in adult ischemia models have demonstrated enhanced angiogenesis/neurogenesis correlating with motor function recovery (Jin et al., 2014; Liu et al., 2014). Given that the developing brain is known to exhibit a greater degree of plasticity (Kolb and Gibb, 2011) and a greater number of resident NPCs compared to the adult brain (Sachewsky et al., 2014), it is plausible that similar mechanisms of enhanced angiogenesis and neurogenesis are occurring in our H/I injury model.

Metformin is a safe, FDA-approved drug, which supports the translation of these findings to the clinic in a reasonable time frame. The therapeutic window for metformin treatment and long-term outcomes, both at the cellular and behavioral levels, will be important considerations for future studies. Further, studies to determine whether metformin treatment can ameliorate cognitive impairments that result following H/I will be important to pursue. Our findings provide compelling support for exploring endogenous NPC activation using metformin for the treatment of childhood brain injury.

EXPERIMENTAL PROCEDURES

Animals

C57/BL6, CD1 pregnant mice were purchased (Charles River Laboratories) and maintained under pathogen-free conditions. CBP S46A and Nestin-CreER^{T2}/R26R-YFP transgenic mice were bred in an animal facility. Tamoxifen at a dose of 0.5 mg/kg was mixed in with rodent chow. All mice were kept on a 12-hr day/night cycle, and procedures were performed in accordance with institutional guidelines approved by the Experimental Animal Committee at the University of Toronto.

H/I Injury Model

Briefly, the left common carotid artery of P8 pups was ligated to give an ischemic insult. Following a 1.5-hr recovery, they were subjected to hypoxia for 1 hr at a temperature of 36°C. Pre-established endpoints were excluded from statistical analysis.

Metformin Administration

For the in vitro neurosphere assay, metformin stock solution was prepared by dissolving in serum-free media (SFMs) and added to culture at various concentrations. In vivo metformin was administered, through a micro-osmotic pump implanted subcutaneously into the mother, at a concentration of 20 mg/kg/day for 7 days. The pups received metformin through the mother's milk. For injection studies, metformin at the above concentration was injected subcutaneously into the pups daily for 7 days.

Neurosphere and Cortical Assay

NSCs were isolated by dissecting the neonatal SE from P8 and P12 animals, as previously described (Morshead et al., 2002), and grown in the presence of mitogens for 7 days. For differentiation assays, individual neurospheres were collected from each condition and plated in the presence of 10% fetal bovine serum (FBS) and the presence and absence of metformin for 7 days. For the cortical assay, the SE was carefully dissected and discarded to ensure no contaminating SE-derived neurospheres were grown in culture. Portions of the cortex were then dissected and processed.

Tissue Preparation and Immunohistochemistry

Animals were sacrificed with an overdose of sodium pentobarbital, perfused with 4% paraformaldehyde at different time points (P8, P16, and P23), and cryoprotected in 20% sucrose overnight at 4°C. Coronal, cryostat sections (20 μm) were mounted on Superfrost Plus slides and stained. Briefly, brain sections were rehydrated for 5 min and permeabilized using 0.3% Triton in PBS for 20 min, rinsed, and then blocked with 1% BSA containing 0.3% Triton in PBS at room temperature. Brain sections were incubated with primary antibodies overnight at 4°C in 1% BSA with 0.3% Triton in PBS. The next day slides were washed and incubated with an appropriate secondary antibody for 2 hr at room temperature, washed, and mounted with DAPI-mounting media. A Zeiss Observer D1 inverted microscope was used to visualize immunofluorescence for differentiated neurospheres and tissue sections. Images were acquired at 20× objective using Axio Vision.

Behavioral Testing

The righting-reflex, hind-limb suspension test was performed as described previously (El-Khodor et al., 2008; Ten et al., 2003). The cylinder-rearing test was used evaluate functional asymmetry resulting from unilateral brain lesion and consequent hemiplegia at P22. Mice were individually placed in a Plexiglas transparent cylinder and video recorded for 4 min or until they reached ten touches per paw. The relative proportion of left (IL) forepaw contacts was calculated as follows: (left − right)/(right + left + both) × 100.

Statistical Analysis

Data were analyzed using Prism Software (version 6, GraphPad). An unpaired Student's t test was used for two-group comparisons. A one-way ANOVA was used for multiple-group comparisons followed by Bonferroni's post hoc test. For analysis comparing CL and IL hemispheres, a two-way ANOVA was performed followed by Tukey's multiple comparisons test. A statistically significant level was defined as $p < 0.05$. Error bars are reported as mean ± SEM unless stated otherwise.

SUPPLEMENTAL INFORMATION

Supplemental Information includes Supplemental Experimental Procedures and two figures and can be found with this article online at http://dx.doi.org/10.1016/j.stemcr.2015.06.011.

AUTHOR CONTRIBUTIONS

P.D. collected, assembled, analyzed, and interpreted data and prepared and approved the manuscript. N.M. and L.S. collected, analyzed, and interpreted data. A.A. collected data. M.F. collected

and analyzed data. F.E.W provided CBP S436A mutant mice. F.D.M. conceived and designed the study. C.M.M. conceived and designed the study; provided financial support; analyzed, interpreted, and assembled data; and wrote and gave final approval of the manuscript.

ACKNOWLEDGMENTS

We thank members of the C.M.M. lab for comments and critical reading of the manuscript. This work was funded by operating grants to C.M.M. from the Stem Cell Network, Three to Be Foundation, Canadian Partnership for Stroke Recovery, the Ontario Brain Institute, and Brain Canada. P.D. was funded by CIHR Training Program in Regenerative Medicine fellowship.

Received: October 31, 2014
Revised: June 27, 2015
Accepted: June 30, 2015
Published: July 30, 2015

REFERENCES

Deng, W. (2010). Neurobiology of injury to the developing brain. Nat. Rev. Neurol. *6*, 328–336.

El-Khodor, B.F., Edgar, N., Chen, A., Winberg, M.L., Joyce, C., Brunner, D., Suárez-Fariñas, M., and Heyes, M.P. (2008). Identification of a battery of tests for drug candidate evaluation in the SMNDelta7 neonate model of spinal muscular atrophy. Exp. Neurol. *212*, 29–43.

Erlandsson, A., Lin, C.H., Yu, F., and Morshead, C.M. (2011). Immunosuppression promotes endogenous neural stem and progenitor cell migration and tissue regeneration after ischemic injury. Exp. Neurol. *230*, 48–57.

Felling, R.J., Snyder, M.J., Romanko, M.J., Rothstein, R.P., Ziegler, A.N., Yang, Z., Givogri, M.I., Bongarzone, E.R., and Levison, S.W. (2006). Neural stem/progenitor cells participate in the regenerative response to perinatal hypoxia/ischemia. J. Neurosci. *26*, 4359–4369.

Hagberg, H., Mallard, C., Ferriero, D.M., Vannucci, S.J., Levison, S.W., Vexler, Z.S., and Gressens, P. (2015). The role of inflammation in perinatal brain injury. Nat. Rev. Neurol. *11*, 192–208.

He, L., Sabet, A., Djedjos, S., Miller, R., Sun, X., Hussain, M.A., Radovick, S., and Wondisford, F.E. (2009). Metformin and insulin suppress hepatic gluconeogenesis through phosphorylation of CREB binding protein. Cell *137*, 635–646.

Ikeda, T., Iwai, M., Hayashi, T., Nagano, I., Shogi, M., Ikenoue, T., and Abe, K. (2005). Limited differentiation to neurons and astroglia from neural stem cells in the cortex and striatum after ischemia/hypoxia in the neonatal rat brain. Am. J. Obstet. Gynecol. *193*, 849–856.

Jin, Q., Cheng, J., Liu, Y., Wu, J., Wang, X., Wei, S., Zhou, X., Qin, Z., Jia, J., and Zhen, X. (2014). Improvement of functional recovery by chronic metformin treatment is associated with enhanced alternative activation of microglia/macrophages and increased angiogenesis and neurogenesis following experimental stroke. Brain Behav. Immun. *40*, 131–142.

Juul, S.E., and Ferriero, D.M. (2014). Pharmacologic neuroprotective strategies in neonatal brain injury. Clin. Perinatol. *41*, 119–131.

Kolb, B., and Gibb, R. (2011). Brain plasticity and behaviour in the developing brain. J. Can. Acad. Child Adolesc. Psychiatry *20*, 265–276.

Kolb, B., Morshead, C., Gonzalez, C., Kim, M., Gregg, C., Shingo, T., and Weiss, S. (2007). Growth factor-stimulated generation of new cortical tissue and functional recovery after stroke damage to the motor cortex of rats. J. Cereb. Blood Flow Metab. *27*, 983–997.

Liu, Y., Tang, G., Zhang, Z., Wang, Y., and Yang, G.Y. (2014). Metformin promotes focal angiogenesis and neurogenesis in mice following middle cerebral artery occlusion. Neurosci. Lett. *579*, 46–51.

Martin-Montalvo, A., Mercken, E.M., Mitchell, S.J., Palacios, H.H., Mote, P.L., Scheibye-Knudsen, M., Gomes, A.P., Ward, T.M., Minor, R.K., Blouin, M.-J., et al. (2013). Metformin improves healthspan and lifespan in mice. Nat. Commun. *4*, 2192.

Morshead, C.M., Benveniste, P., Iscove, N.N., and van der Kooy, D. (2002). Hematopoietic competence is a rare property of neural stem cells that may depend on genetic and epigenetic alterations. Nat. Med. *8*, 268–273.

Ong, J., Plane, J.M., Parent, J.M., and Silverstein, F.S. (2005). Hypoxic-ischemic injury stimulates subventricular zone proliferation and neurogenesis in the neonatal rat. Pediatr. Res. *58*, 600–606.

Plane, J.M., Liu, R., Wang, T.W., Silverstein, F.S., and Parent, J.M. (2004). Neonatal hypoxic-ischemic injury increases forebrain subventricular zone neurogenesis in the mouse. Neurobiol. Dis. *16*, 585–595.

Romanko, M.J., Rothstein, R.P., and Levison, S.W. (2004). Neural stem cells in the subventricular zone are resilient to hypoxia/ischemia whereas progenitors are vulnerable. J. Cereb. Blood Flow Metab. *24*, 814–825.

Sachewsky, N., Leeder, R., Xu, W., Rose, K.L., Yu, F., van der Kooy, D., and Morshead, C.M. (2014). Primitive neural stem cells in the adult mammalian brain give rise to GFAP-expressing neural stem cells. Stem Cell Reports *2*, 810–824.

Ten, V.S., Bradley-Moore, M., Gingrich, J.A., Stark, R.I., and Pinsky, D.J. (2003). Brain injury and neurofunctional deficit in neonatal mice with hypoxic-ischemic encephalopathy. Behav. Brain Res. *145*, 209–219.

Vannucci, R.C., and Vannucci, S.J. (2005). Perinatal hypoxic-ischemic brain damage: evolution of an animal model. Dev. Neurosci. *27*, 81–86.

Vannucci, R.C., Connor, J.R., Mauger, D.T., Palmer, C., Smith, M.B., Towfighi, J., and Vannucci, S.J. (1999). Rat model of perinatal hypoxic-ischemic brain damage. J. Neurosci. Res. *55*, 158–163.

Venna, V.R., Li, J., Hammond, M.D., Mancini, N.S., and McCullough, L.D. (2014). Chronic metformin treatment improves post-stroke angiogenesis and recovery after experimental stroke. Eur. J. Neurosci. *39*, 2129–2138.

Wang, J., Weaver, I.C.G., Gauthier-Fisher, A., Wang, H., He, L., Yeomans, J., Wondisford, F., Kaplan, D.R., and Miller, F.D. (2010). CBP histone acetyltransferase activity regulates embryonic neural differentiation in the normal and Rubinstein-Taybi syndrome brain. Dev. Cell *18*, 114–125.

Wang, J., Gallagher, D., DeVito, L.M., Cancino, G.I., Tsui, D., He, L., Keller, G.M., Frankland, P.W., Kaplan, D.R., and Miller, F.D. (2012). Metformin activates an atypical PKC-CBP pathway to promote neurogenesis and enhance spatial memory formation. Cell Stem Cell *11*, 23–35.

Yang, Z., and Levison, S.W. (2006). Hypoxia/ischemia expands the regenerative capacity of progenitors in the perinatal subventricular zone. Neuroscience *139*, 555–564.

Yang, Z., Covey, M.V., Bitel, C.L., Ni, L., Jonakait, G.M., and Levison, S.W. (2007). Sustained neocortical neurogenesis after neonatal hypoxic/ischemic injury. Ann. Neurol. *61*, 199–208.

Zaidi, A.U., Bessert, D.A., Ong, J.E., Xu, H., Barks, J.D., Silverstein, F.S., and Skoff, R.P. (2004). New oligodendrocytes are generated after neonatal hypoxic-ischemic brain injury in rodents. Glia *46*, 380–390.

Stem Cell Reports, Volume *5*

Supplemental Information

Activating Endogenous Neural Precursor Cells Using Metformin Leads to Neural Repair and Functional Recovery in a Model of Childhood Brain Injury

Parvati Dadwal, Neemat Mahmud, Laleh Sinai, Ashkan Azimi, Michael Fatt, Fredric E. Wondisford, Freda D. Miller, and Cindi M. Morshead

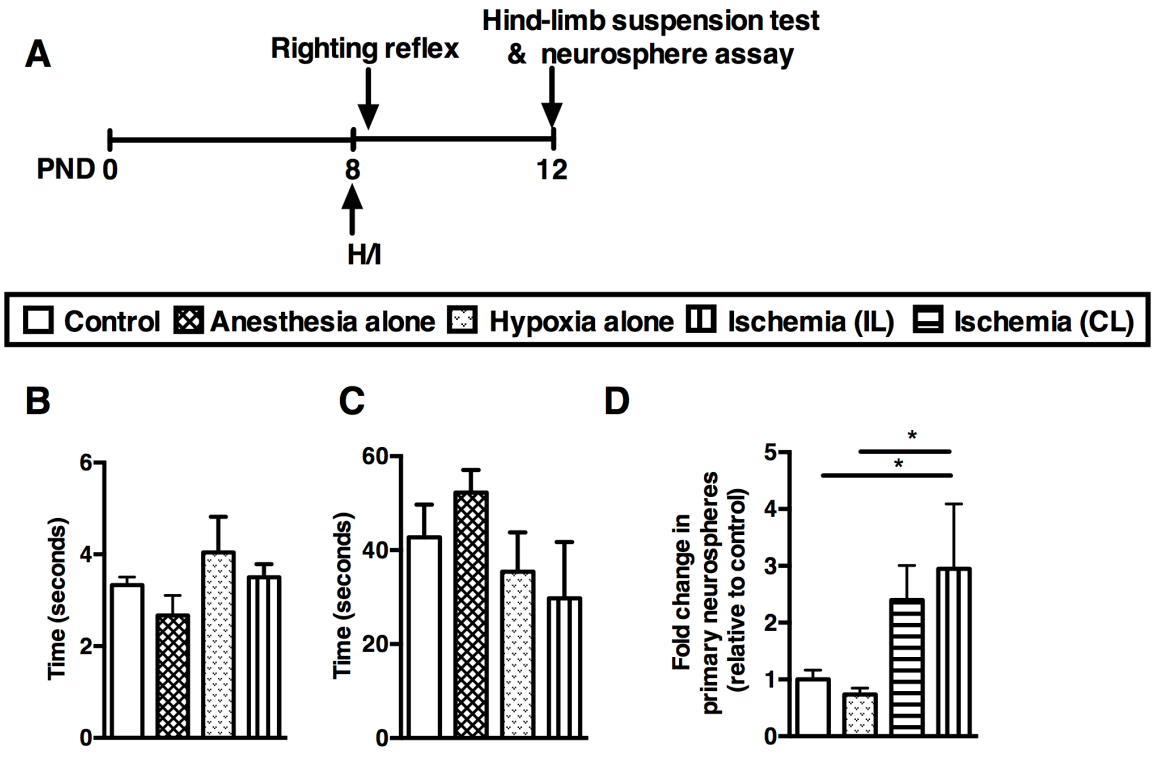

Supplemental Figure 1

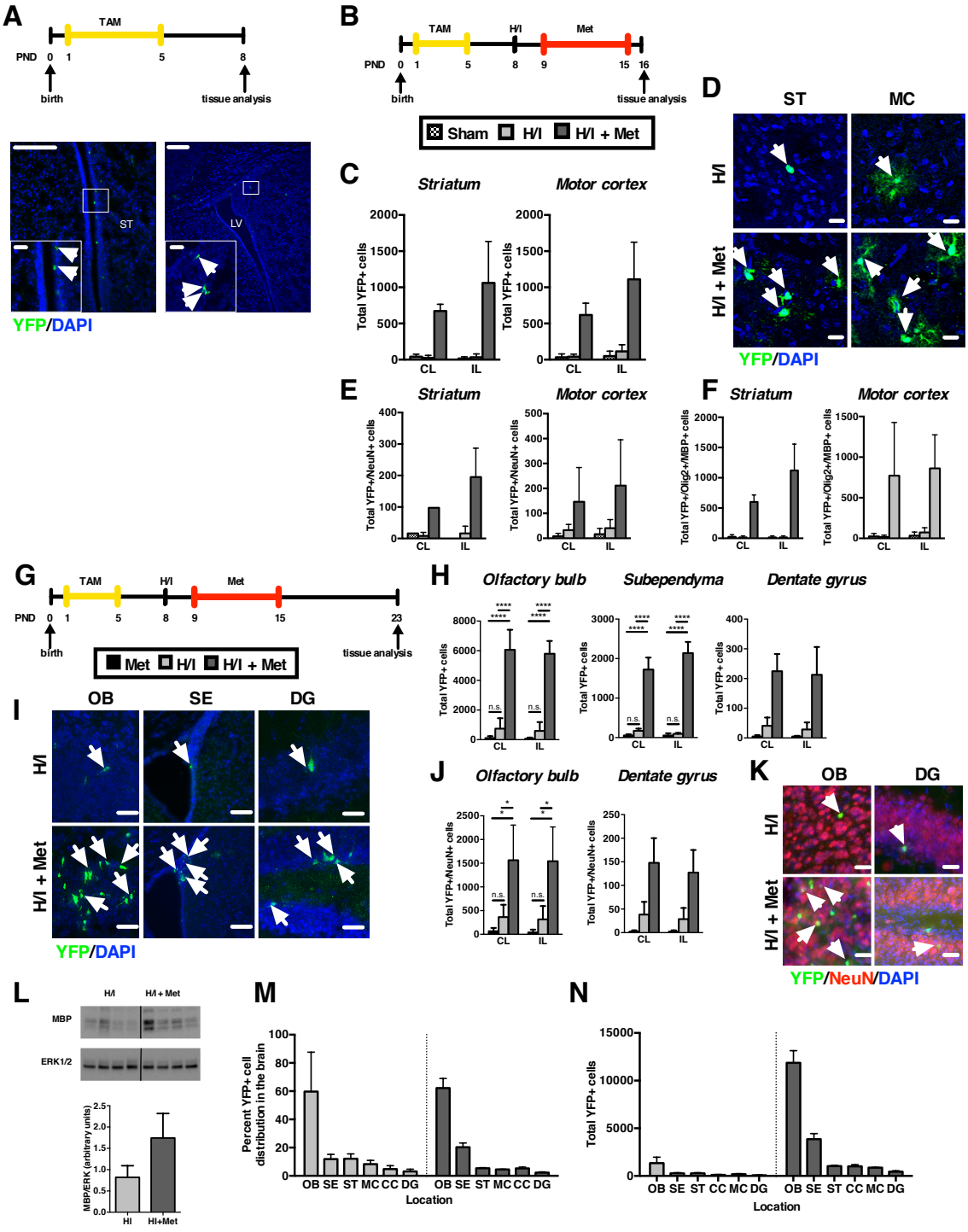

Supplemental Figure 2

Supplemental Figure Legends

Figure S1. Behavioral assessment and examining endogenous NPCs in hypoxia injured and ischemia injured mice. **(Related to Figure 2)** (A) Experiment paradigm for H/I model. (B) Righting reflex was tested on mice one hour after injury ($n \geq 4$ mice/group, one-way ANOVA) (C) Four days after H/I, the hind-limb suspension test was performed ($n \geq 4$ mice/group, one-way ANOVA). (D) Pups that received ischemia alone had an increase in the numbers of neurospheres on the ipsilateral (ischemic) hemisphere when compared to uninjured controls and hypoxic mice following four days of recovery ($n \geq 4$ mice/group, one-way ANOVA). Error bars represent mean ± s.e.m. *$P < 0.05$

Figure S2. Lineage tracing *in vivo*. (Related to Figure 3) (A) *Nestin-creER^{T2}/R26R-YFP* dams received tamoxifen in food chow and pups obtained tamoxifen through the mother's milk prior to H/I. At PND 8, the majority of the YFP+ cells (nestin expressing) were found in the lining of the lateral ventricles, with a few cells in the parenchyma, including the olfactory bulb and rostral migratory stream, in tamoxifen fed pups. Scale bars = 100 μm and insets are 20 μm (B) Experimental paradigm immediately after metformin treatment (PND 16). (C) Quantification of YFP+ cells in striatum and motor cortex ($n = 2$ mice/group) at PND 16. Sham-operated controls underwent anesthesia and incision but no artery occlusion or hypoxia. (D) SE-derived YFP+ cells (green) and Hoechst (blue). Quantification for (E) YFP+/NeuN+ neurons and (F) YFP+/MBP+ and YFP+/Olig2+ in striatum and motor cortex at PND 16 ($n = 2$ mice/group). (G) Experimental paradigm at the time of functional recovery (PND 23). (H) Quantification

of YFP+ cells in granule cell layer of the OB ($n \geq 3$ mice/group with the exception of metformin alone where n=2, two-way ANOVA), subependyma ($n \geq 3$ mice/group, two-way ANOVA) and dentate gyrus ($n \geq 3$ mice/group, two-way ANOVA), 2 weeks post H/I. (I) Coronal sections were immunostained for SE-derived YFP+ cells (green) and Hoechst (blue). (J) Quantification of YFP+ cells that were co-labeled with NeuN indicating newborn neurons in olfactory bulb ($n \geq 3$ mice/group with the exception of metformin alone where n=2, two-way ANOVA) and dentate gyrus ($n \geq 3$ mice/group, two-way ANOVA). (K) Coronal sections were immunostained for SE-derived YFP+ cells (green), NeuN (red) and Hoechst (blue). (L) Western blot (*top*) and densitometric analysis (*bottom*) of MBP expression in the ipsilateral motor cortex on PND 23 following either H/I or H/I with metformin treatment (H/I + Met), as outlined in G (n =4 mice/group). (M) Distribution of SE-derived precursors at PND 23. Graph depicts, the relative YFP+ cell distribution in the brain as a percentage of total YFP+ cells. Metformin treatment did not change the location of where newborn cells are found in the brain. IL and CL hemisphere were pooled together ($n \geq 4$ mice/group/area with the exception of OB and SE counts for H/I+ Met where n =3; two-way ANOVA). (N) Total YFP+ cells labeled at PND 23. IL and CL hemisphere were pooled together ($n \geq 4$ mice/group/area with the exception of OB and SE counts for H/I+ Met where n =3). Arrows denote labeled cells. Scale bars = 20 μm. Met = metformin, CL = contralateral hemisphere, IL = ipsilateral hemisphere, OB = olfactory bulb, SE = subependyma, DG = dentate gyrus, ST = striatum, MC = motor cortex, CC = corpus callosum. Error bars represent mean ± s.e.m. with the exception of (H, olfactory bulb) and (J, olfactory bulb) where error bars represent mean ± s.d. $*P < 0.05$, $**** P < 0.0001$

Supplemental Experimental Procedures

Mice. C57BL/6 pregnant mice were purchased from Charles River. In a pathogen free facility, a dam was housed in a single cage with a red rectangular/dome house, one nestlet, with food and water available *ad libitum.* Neonates at PND 8 and PND 12 (both males and females) were sacrificed and used for the neurosphere assay. CBPS436A mice, a kind gift from Dr. Miller's lab, were genotyped and used for the neurosphere assay at PND 8 and PND 12 (both males and females). For lineage tracing experiments, *Nestin-CreER^{T2}/R26R-YFP* mice were bred in animal facility and offspring genotyped. At time of birth, *Nestin-CreER^{T2}/R26R-YFP* neonates (both males and females) were cross-fostered to a CD1 lactating mother (Charles River) and provided with a red rectangular/dome house and one nestlet per cage. Foster mothers received tamoxifen in food chow (approximately 5 pellets) and this was delivered to *Nestin-CreER^{T2}/R26R-YFP* neonates (through the mother's milk) to induce Cre recombination from PND1 until PND 5. Briefly, tamoxifen (Sigma-Aldrich, St. Louis, MO) at a concentration of 250 mg/kg was mixed with high fat food (2019, Harlan), 0.5% sucrose and green food coloring and manufactured as pellets by Harlan laboratories. Food chow was then changed to high fat diet for the remainder of the experiment. The brains of these animals were perfused on PND 8, 16 and PND 23. All mice were kept on a 12-hour day/night cycle. All procedures were performed in accordance with institutional guidelines and approved by the Experimental Animal Committee at the University of Toronto.

Hypoxia/Ischemia injury model. Briefly, PND 8 pups (2 – 4 g) were anesthetized (isoflurane, 5% induction and 1.5% maintenance) and under a surgical microscope (Möller Hi-R 900) the left common carotid artery was ligated using sutures (Sofsilk, VS889). Bupivacaine (0.25 mg/mL) was administered once intra-operation for local

analgesia. The duration of anesthesia was <15 minutes. Following surgical procedure, neonates were kept under the heat lamp for 15 minutes and then returned to the dam for 1-2 hours of recovery. Neonates were then placed in a plastic container, submerged in a water bath and subjected to hypoxia (8% O_2 in N_2) for 1 hour at a temperature of 36 °C. Pre-established endpoints for exclusion from the study were mice that demonstrated hunched or abnormal posture, lethargy or reluctance to move, hypothermia, persistent anorexia and dehydration. Injured mice demonstrating typical H/I lesions (i.e. striatal atrophy and enlargement of the ipsilateral ventricle) at PND 23 time point were included in analysis, as described previously (Plane et al., 2004).

Metformin administration. For the neurosphere assay, a stock solution of metformin (0.167 mg/mL, Sigma-Aldrich, D150959) was made by dissolving in serum free media (SFM) and subsequently adding to various concentrations in culture. In our *in vivo* studies, a daily dose of metformin at a concentration of 20 mg/kg/day was dissolved in 1x PBS and delivered by implanting a subcutaneous micro-osmotic one week pump (Alzet, 10070) to lactating mothers. Briefly, mothers were anesthetized using isoflurane and injected with ketoprofen i.p. (0.1 mg/10 g body weight) for analgesia. A small incision was made and the pump was implanted on the side and sutured (Sofsilk, 2613-SS683G). Mothers then recovered under the heat lamp and were returned to their litter. For the PBS/metformin injection studies, a daily record of the weights was kept. Pups were injected subcutaneously, once daily from PND 9-15 using a 30G ½ needle with a maximum volume of 50 µL.

Neurosphere assay. Neural stem cells were isolated by dissecting the neonatal SE of PND 8 and PND 12 animals. Briefly, tissue was digested with enzymes (1.33 mg/mL

trypsin, 0.67 mg/mL hyaluronidase, and 0.2 mg/mL kynurenic acid, (Sigma- Aldrich) for 10 min at 37°C. Enzyme activity was inhibited with trypsin inhibitor (0.67mg/mL, Roche Diagnostics). Tissue was mechanically dissociated into a single-cell suspension and plated at clonal density (5 cells/µl)(Coles-Takabe et al., 2008) in 24-well polystyrene plates (VWR Scientific) with serum-free medium (SFM) containing 1% penicillin/streptomycin (Invitrogen) and supplemented with epidermal growth factor (20 ng/mL, Sigma-Aldrich), basic fibroblast growth factor (10 ng/mL, Sigma-Aldrich), heparin (7.35 ng/mL, Sigma-Aldrich). Neurospheres ≥ 80 µm in diameter were quantified 7 days later. For differentiation assays, individual neurospheres were collected from each condition (approximately 150-200 µm), gently triturated, and plated onto laminin (L2020, Sigma-Aldrich) coated 48 well plates (VWR Scientific) in the presence of 10% fetal bovine serum (10082139, Invitrogen) and in the presence and absence of metformin for 7 days.

Cortical assay. The SE was carefully dissected and discarded to ensure no contaminating SE-derived neurospheres were grown in culture. Portions of the striatum and motor cortex were then dissected and processed as described above. Neurospheres were counted on day 7.

Immunofluorescence and antibodies. Animals were sacrificed with an overdose of sodium pentobarbital, perfused with 4% paraformaldehyde at different time points (PND 8, 16 and 23) and cryoprotected in 20% sucrose overnight at 4°C. Coronal, cryostat sections (20 µm) were mounted on Superfrost Plus slides and stained. Briefly, brain sections were rehydrated for 5 minutes and permeabilized using 0.3% triton in PBS for 20 minutes, rinsed, and then blocked with 1% BSA containing 0.3% triton in PBS at

room temperature. Brain sections were incubated with primary antibodies overnight at 4°C in 1% BSA with 0.3% triton in PBS. The next day slides were washed and incubated with an appropriate secondary antibody for 2 h at room temperature, washed and mounted with DAPI mounting media. The primary antibodies used were O4 (1:1000 mouse monoclonal IgM, R&D Systems, MAB1326), βIII-tubulin (1:1000, rabbit polyclonal, Covance, PRB-435P-100), GFP (1:500, chicken IgY, Aves Lab, GFP-1020), Olig2 (1:200, rabbit polyclonal, Millipore, AB9610), MBP (1:50, rat monoclonal, Abcam, AB7349), NeuN (1:100, mouse monoclonal IgG, Millipore, MAB377), NeuN (1:500, rabbit monoclonal IgG, Cell Signaling, 12934). The secondary antibodies used were AlexaFluor 488, AlexaFluor 568, AlexaFluor 594, AlexaFluor 647 conjugated goat anti-mouse IgM, goat anti-rabbit IgG, goat anti-chicken, donkey anti-rat IgG, goat anti-mouse IgG (Invitrogen).

Microscopy and cell counting. A Zeiss Observer D1 inverted microscope was used to visualize immunofluorescence using YFP (500 nm excitation; 535/50 emission filter), Texas Red (560 nm excitation; 630/75 emission filter), Cy5 (620 nm excitation; 700/75 emission filter) for differentiated neurospheres and tissue sections. Images were acquired at 20x objective using Axio Vision (version 4.8.1.0). For differentiation of neurospheres, cells were counted within the field of view in five areas [top, bottom, left side, right side (all equal distance from the edge of the well) and center]. Percentages of differentiated cells were calculated to the total numbers of cells in each field of view and plotted as fold increase. In tissue sections, quantification was performed for the ipsilateral and contralateral hemispheres for all analysis. The total number of cells per section was counted in every 5^{th} section and multiplied by the total number of sections per region.

Counts for the corpus callosum, motor cortex, striatum and SE began were as described previously(Morshead et al., 1998). The granular cell layer in the OB and the DG in the hippocampus were also counted.

Western blot. The motor cortex was dissected from H/I and H/I + metformin treated brains at PND 23. This region was then lysed in Radioimmunoprecipitation assay (RIPA) buffer supplemented with 2 μg/ml Aprotinin, 10 μg/ml Leupeptin, 1mM PMSF, 10mM Sodium Fluoride, and 1mM Sodium Orthovanadate. Equal amounts of protein (15 μg) per sample were run on Mini-PROTEAN TGX Gels (4-20%, BioRad, Hercules, CA), transferred to 0.2-μm nitrocellulose membranes, blocked for 30 min with 5% non-fat dry milk, 0.1%Tween-20 in TBS, and incubated overnight at 4 °C with primary antibody in blocking buffer. After washing several times with 0.1%Tween-20 in TBS, membranes were incubated for 1 h at room temperature with the following secondary antibodies: goat anti-rat (1:5000, Life Technologies) and goat anti-rabbit (1:10 000, Life Technologies). After several more washes, detection was performed using ECL chemiluminescence reagent (GE Healthcare, Buckinghamshire, UK). The following primary antibodies were used: rat anti-MBP (MCA409S, 1:1000, ABD Serotec, Raliegh, NC) and rabbit anti-ERK1 (K-23, 1:10 000, Santa Cruz Biotechnology, Santa Cruz, CA).

Behavioral testing

Righting reflex. One hour after H/I, PND 8 mice were tested on the righting reflex. Animals were placed on supine position and the time to turn into prone position was measured as described previously (Ten et al., 2003). Pups were allowed three attempts to perform the reflex for up-to 60 seconds per attempt and the mean time was recorded.

Hind-limb suspension test. Four days post H/I, PND 12 mice were tested on the hind-limb suspension test as described previously (El-Khodor et al., 2008). Briefly, mice are placed head-down, hanging by their hind limbs on the edge of a plastic 50 mL falcon tube with tissue at the bottom to protect the head of the pups upon their fall into the tube. The latency to fall from the edge of the tube was assayed over a 60 s period.

Cylinder rearing test. To evaluate functional asymmetry resulting from unilateral brain lesion and consequent hemiplegia, the cylinder test was performed at 22 days of age. Mice were individually placed in a Plexiglas transparent cylinder (7.5 cm x 15 cm height) and video recorded for 4 minutes or until they reached 10 touches per paw. Initial forepaw (left/right/both) preference of weight-bearing touches during a rear was recorded. The relative proportion of left (ipsilateral) forepaw contacts was calculated as: (left – right) / (right + left + both) x 100. Sham animals showed no preference for either right or left fore-paw initiation but H/I injured animals demonstrated a preference in using the left forepaw depending on the severity of the insult.

Statistical analysis. Data were analyzed using Prism Software (Graphpad, Version 6). An unpaired Student's t-test was used for two group comparisons. A one-way ANOVA was used for multiple group comparisons followed by Bonferroni's post-hoc test. For analysis comparing contralateral and ipsilateral hemispheres a two-way ANOVA was performed followed by Tukey's Multiple comparisons test. A statistically significant level was defined as $P < 0.05$. Error bars are reported as mean ± s.e.m unless stated otherwise.

Supplemental References

Coles-Takabe, B.L., Brain, I., Purpura, K.A., Karpowicz, P., Zandstra, P.W., Morshead, C.M., and van der Kooy, D. (2008). Don't look: growing clonal versus nonclonal neural stem cell colonies. Stem Cells *26*, 2938–2944.

Morshead, C.M., Craig, C.G., and van der Kooy, D. (1998). In vivo clonal analyses reveal the properties of endogenous neural stem cell proliferation in the adult mammalian forebrain. Development *125*, 2251–2261.